

Deforestation and Secondary Growth in Rondonia, Brazil from SIR-C SAR and Landsat/SPOT Data

Eric Rignot, William A. Salas*, and David L. Skole*

Jet Propulsion Laboratory, California Institute of Technology, 4800 Oak Grove
Drive, Pasadena CA 91101-8099.

* Institute for the Study of Earth, Oceans and Space, University of New Hampshire,
Durham, NH 03824

Abstract. Excellent data on deforestation have been obtained in the tropics using high-resolution optical sensors. Yet, several problems remain. Cloud cover creates data gaps which limit the possibility of complete and frequent assessments, and secondary growth is not well characterized. Active microwave sensors could usefully complement these sensors because they operate independent of cloud cover and are more prone to detect differences in woody biomass associated with various stages of clearing and regrowth. An example is discussed here using fully polarimetric, C- (5.6 cm) and L-band (24 cm) frequency radar data gathered in October 1994 by NASA's Shuttle Imaging Radar C (SIR-C), south-east of the city of Porto Velho, in the state of Rondonia, Brazil. We analyzed the SIR-C data in combination with Landsat TM data acquired in October 1993, a 9-year time series of SPOT XS data acquired in July-August from 1986 to 1991, and a preliminary field survey conducted in October 1995. L-band polarimetric radar data separate well primary forest, non-forest, and various stages of forest clearing and vegetation re-growth of different woody biomasses. They do not separate well intermediate regrowth 7-8 years of age. Recent clearings are radar-bright, at horizontal polarization due to the presence of felled and standing dead trunks, and decrease in brightness with age. Landsat TM / SPOT XS separate well primary forest, deforested areas, and forest regrowth, but provide little information on vegetation biomass. Significant improvements in land cover classification arise from combining Landsat TM 1993 and SIR-C 1994 data. We separate with a high degree of confidence: 1) open water; 2) flooded dead forest; 3) primary forest; 4) clearings with 110 woody biomass; 5) 1-year-old slash and burn of intermediate woody biomass; 6) <1-year-old slash and burn of high woody biomass; 7) initial secondary growth (0-5 years) of low woody biomass; and 8) intermediate secondary growth (6-9 years) of intermediate woody biomass. The results demonstrate the synergy between radar and optical for detecting various levels of woody biomass and live vegetation in secondary growth. Current prospects with existing international SARs are limited. C-band SARs are inappropriate for detecting woody biomass. At our site, JERS-1, single-channel, L-band SAR underestimates deforestation by >100% because it does not separate well intermediate levels of woody biomass. SARs operating at long radar wavelengths, with both like and cross-polarizations, are needed for tropical deforestation studies.

Introduction and Objectives

Over the last two centuries, the concentration of atmospheric carbon dioxide has increased by > 25% (Neftci et al., 1985). Most of the current flux is attributed to fossil fuel burning, but a third is thought to have come from deforestation in the tropics (Houghton, 1991; Houghton and Skole, 1990; Houghton et al., 1985). Although it is generally agreed that tropical land use change is a net source of atmospheric carbon, estimating the magnitude of this source is difficult. Three types of data are required to calculate its magnitude: 1) the rates and geographic distribution of deforestation, 2) the fate of deforested land, including regrowth and re-clearing, and 3) the changes in the stocks of carbon above and below ground as a result of disturbance and recovery time. Although the rate and extent of deforestation have become more accurately documented in recent years, large uncertainties remain in the estimates of carbon stocks in soil and vegetation (Houghton, 1991) and in the fate of deforested land (Skole et al., 1994).

Satellite remote sensing has helped quantify deforestation over large regions (Tucker et al., 1984; Nelson and Holben, 1986; Nelson et al., 1987; Skole and Tucker, 1993). Although initial estimates diverged widely, they converged in recent years as a result of a wider utilization of high-resolution (< 100 m) sensors (Townshend and Justice, 1988; Skole et al., 1994; Moran et al., 1994). Excellent data on deforestation has been obtained and are being obtained with Landsat images over the entire legal Amazon (Skole and Tucker, 1993) and in south-east Asia through NASA's Landsat Pathfinder program (Skole, pers. commun. 1996). Forest, clearings, and secondary growth are well separated spectrally. Yet, several problems remain. First, the various stages of secondary regrowth are not easily differentiated. Second, cloud cover is an ubiqui-

tous problem in the humid tropics which limits deforestation assessments in time and space. Third, optical sensors are not good tools for measuring stand characteristics such as density and biomass (Sader et al., 1989). As a result, deforestation assessments are conducted over periods of several years, gaps exist in ground coverage, and information on woody biomass and accumulation rate of secondary growth is limited and site specific..

Carbon models often ignore the role of secondary forests because it is not well known what fraction of the landscape they occupy, how much carbon they accumulate and how quickly, and what fraction of deforestation occurs in secondary growth. Secondary forests have lower stocks of earlml, but they accumulate carbon quickly in the 10-20 years following disturbances (Brown and Lugo, 1990). In one area of Rondonia, Brazil, Skole et al. (1994) estimated 30 percent of the disturbed forests were secondary growth, and the pool of regrowth doubled between 1986 and 1989 (Alves and Skole, 1996). Each year, 50 percent of the deforested land is abandoned, and 42 percent of new clearings were from secondary growth in 1988-89 (Skole et al., 1994).

Separating different ages of regrowth is possible with multi-year optical data (Lucas et al., 1993, Moran et al. 1994, Adams et al., 1995, Steininger, 1996) but the task over the entire Amazon basin would be daunting. These multi-year techniques are site-specific, limited by the availability of cloud-free images, and provide little information on woody biomass. One alternative is to combine optical with radar data. The interest of the synergy emerged years ago (Stone and Woodwell, 1982), but the prospects have been limited by the absence of spat. etx mle SARs and by the lack of airborne SAR observations of the tropics, until just recently. Radar systems have several inherent advantages that make them a unique complement to optical sensors. They operate

independent of solar illumination and cloud cover, and interact with the larger-sized components of the forest, such as branches and tree-trunks, which contain the largest fraction of woody biomass. Research conducted in the late 1980's and early 1990's, on non-tropical forests, with airborne radar sensors showed radars perform best at measuring woody biomass when operating at the longer radar wavelengths, at more than one polarization (e.g. Sader, 1987; Dobson et al., 1992; Rignot et al., 1995).

The data collected in 1994 by NASA's Shuttle Imaging Radar C (SIR-C) during its two missions were by far the most comprehensive data set of multi-channel radar observations ever collected in the tropics. Its overflight of South America provided the first synoptic views of the Amazon basin at both C- (5.6 cm) and L-band (24 cm) frequency, with multiple polarizations, over regions long surveyed by optical sensors. Our study site is located in the state of Rondonia, Brazil, within an area selected for intensive studies of tropical deforestation for the Landsat Pathfinder project (Chomentowski et al., 1994), along a track for which fully polarimetric radar data were collected. The availability of full polarimetry is an important advantage over single or dual-channel data because it provides a complete characterization of radar scattering at a given radar wavelength. It is then possible to analyze separately the contributions from surface scattering, volume scattering, or double bouncing of the radar signals. This analysis helps in turn better interpret the type of ecological information obtainable from the radar data, resolve uncertainties in interpretation of single or dual-channel data, and predict the performance level of existing and/or future SARs. To validate the results, we employed Landsat TM imagery from 1993 and SPOT XS imagery from 1986, 1988, 1989, 1991, 1992, and 1994 (no cloud-free data were collected in 1987, 1990, and 1993). We conducted a preliminary field survey of the site in October 1995. We now describe the performance of SIR-C SAR at detecting

deforestation and the fate of deforested land, the synergistic utilization of SIR-CSAR and Landsat TM, and the prospects for future combined use of the two technologies.

Study Site

Our study site is located 50 km south-east, of Porto Velho, the capital of the state of Rondonia, in a region of low relief, with gently rolling topography, high precipitation and tropical seasonal climate. Deforestation has increased in Rondonia at a faster rate over the past two decades than anywhere else in the world (Malingreau and Tucker, 1988). Colonization and agricultural expansion programs started in 1968 and accelerated greatly in 1984 with the completion of highway 111-364 which facilitated immigration into Rondonia. The region once supported a continuous cover of primary tropical moist rain forest, with a woody biomass of about 170 tons of carbon per hectare (Brown and Lugo, 1990). About 12 percent of the Rondonia forests have been cleared in the 1980's (Skole et al., 1994), where there was little deforestation in the 1970's. The majority of clearings are established by felling and burning of the forest, mostly by families (Dale et al., 1994). Much of the land is now in pasture of various quality for cattle, and secondary growth of various ages. Smaller plots are planted with coffee, maize, beans and other crops (Dale et al., 1994). Unproductive fields are quickly abandoned, typically after 3-4 years, to support forest regrowth (Alves and Skole, 1996). Regrowth is typically vigorous and dominated by several pioneer species (e.g. *Cecropia*), which yield a regular and homogeneous canopy structure. The rates of accumulation of biomass (a net uptake of atmospheric carbon) depend on the age of forest clearing, but also on the history and intensity of land use prior to abandonment (Uhl et al., 1988; Nepstad et al., 1991).

Remote Sensing Data

The SIR-C imagery available for our site was limited to a single track named Manaus CSAP-B, Brazil, acquired on October 6, 1994 at 06:18:28.1 GMT or 02:18 am local time, during orbit 94 of the space shuttle Endeavour. The false-color composite image shown in Figure 1 is centered at 8 deg 58' south, 63 deg 17' west. North is on top. Image size is 20.7 km by 25 km. Pixel spacing is 12.5 m and spatial resolution is 25 m on the ground in both along-track (azimuth) and across-track (range) direction. SIR-C illuminated the scene from the right, at an altitude of 213 km, with an incidence angle of the radar illumination at scene center of 37°. The data were automatically calibrated in the JPL SIR-C SAR processor. In Figure 1, red is the radar amplitude measured at L-band frequency (24 cm) HH-polarization (horizontal receive and transmit); green is L-band HV-polarization (horizontal receive and vertical transmit); and blue is C-band (5.66 cm) frequency, HV-polarization. The SIR-C images were spatially registered to the Landsat TM images after rotation and re-sampling of the SAR imagery to a common pixel spacing on the ground, and using precision tie-pointing between the two scenes.

A JERS-1 SAR scene of the same region was acquired in February 1994 (Figure 2). The sensor altitude was 580 km, with the same incidence angle as SIR-C. Spatial resolution was only 100 m in the product made available to us.

One cloud-free Landsat TM scene was acquired on October 7, 1993. Spatial resolution is 30 m. In Figure 3, red is the reflectance measured in band 4 (near infra-red), green is band 3 (red visible), and blue is band 5 (mid infra-red). Areas of old-growth forest appear blue, secondary growth is red, and primary forest has an intermediate darker red signature.

Multispectral SPOT XS data from 1986, 1988, 1989, 1991, 1992 and 1994 were also

available for that area. Spatial resolution is also 30 m. The spectral bands are different from those on Landsat TM. SPOT has green visible, red visible and near infra-red channels, but no mid infra-red channel. All SPOT data were acquired in July-August, after most forest clearing has occurred. Landsat TM and SIR-C data were acquired in early October which coincides with the peak of the burning season.

Preliminary field survey

We visited the test site in late October 1995, one year after the SIR-C flight. Forest clearings which occurred in the summer of 1995 could, however, easily be identified in the field because of the fire scars. Visiting the area with satellite imagery in hand and a preliminary analysis of the data also helped optimize the field selection, the type of observations to be made, and the positioning and navigation from one field to the next.

Ground photographs were taken in all four directions in the 24 emplacements we visited. Representative examples of the types of land cover are given in Figure 4. We noted GPS location, major types of land cover (pasture, forest, succession forest, slash and burn, etc.) and, whenever possible, estimated the approximate age of clearings based on ground cover and land degradation]. A more detailed and extensive field campaign is planned in the area in the summer of 1996.

Methods

The SPOT XS images were analyzed to estimate the age of clearings of about 150 fields, and the history of land use between 1986 and 1994. Only four categories of land cover were utilized: water, forest, Holl-forest, and secondary growth. These are the same categories which are operationally utilized for the Landsat Pathfinder

(1,1') project (Chomentowski et al., 1994). The classification technique used for the Landsat TM data was an iterative self-organizing data analysis technique (Tou and Gonzalez 1974) to define the inherent spectral clusters (40 clusters) within the data. A convergence threshold of 95 required to meet this threshold. A minimum distance classifier was applied to assign the pixels to the clusters. A knowledge-based approach was used to assign the output clusters to our thematic classes of water, forest, Joll-forest and secondary growth (Figure 5).

To classify the SIR-C data, we selected training sites in the various types of land cover visually separated in the false-color composite Sill-C image. Labeling of these training sites into various types of land cover was performed based on the results of the Landsat classification, the field survey, and our knowledge of radar scattering from land surfaces. We selected one training area for each one of the 7 categories of land cover that could be identified in the SIR-C image. These categories are: 1) open water; 2) flooded dead forest; 3) primary forest; 4) clearings with no woody biomass; 5) recent slash and burn with high woody biomass; 6) older slash and burn of lower woody biomass; and 7) initial secondary growth. To classify the entire scene, the Bayesian classifier of Rignot and Chellappa (1992) was utilized. The polarimetric characteristics of the training sites are listed in Table 1. The SIR-CSAR classification map is shown in Figure 6.

To help understand and physically interpret the radar scattering properties of the scene, we used a mathematical decomposition of the polarimetric signal into canonic forms of scattering (van Zyl, 1992). Total backscatter from the polarimetric data is decomposed into its eigenvalues and eigenvectors which correspond to three scattering modes: 1) single bounce scattering; 2) double bounce scattering, and 3) volume scat-

tering. Single bounce scattering is represented in blue in Figure 7, double bouncing is red, and volume scattering is green. The intensity of each color is proportional to the contribution of each canonic form of scattering to total backscatter. The results are discussed in the next section.

Results

Analysis of Radar Scattering

In the Cloude decomposition, volume scattering (green) dominates the landscape at both radar frequencies (Figure 7). The magnitude of volume scattering is determined by the intensity of the cross-polarized returns (van Zyl, 1992). Scattering models of forest canopies showed cross-polarized returns are caused by volume scattering interactions with the branches and leaves of the forest canopy (Durdnet al., 1989; van Zyl, 1989), and therefore depend mostly on crown biomass, the dielectric constant of the tree constituents (meaning essentially their water content) and canopy structure. At C- and L-band, radar backscatter of primary forests is therefore dominated by volume scattering interactions within the forest canopy. Other sources of scattering, which include single bouncing of the signals on the ground or on the upper canopy and double-bounce mechanisms between trunk-ground or canopy-ground reflectors, are much less significant. The "greenness" of the decomposition is also larger at C- than at L-band. This is an expected result because C-band signals interact mostly with randomly oriented objects from the upper canopy (leaves, twigs, and branches), whereas L-band signals interact more with larger, less randomly oriented, objects such as the larger branches.

Over flooded dead forests bordering the Rio Jamari, double bouncing of the radar

signals dominates. These forests were killed by permanent river flooding after the completion of Samuel Dam in 1989. We attribute their radar signature to double bouncing of the radar signals on the corner reflectors formed by the dead tree-trunks standing in flooded ground. Volume scattering is limited because no live forest canopy is present, and surface scattering is limited because radar signals bounce away from the radar direction when they reach the highly reflective flooded ground. Double bouncing is facilitated by the lack of attenuation of the incoming radar signals by the forest canopy. These forests are the brightest objects of the entire scene.

Over clear-cuts, the blue color dominates, which is consistent with single bounce scattering on a dielectric surface. The proportion of volume scattering increases at C-band compared to L-band, probably the result of enhanced scattering from a vegetation layer of shrubs and grasses at C-band.

Recently cleared areas behave differently from any other type of land cover. Double bouncing, single bouncing and volume scattering contribute almost equally to total backscatter, resulting in a nearly white tone in Figure 7, especially at L-band. Double bouncing of the radar signals on the remaining standing trunks is therefore not the dominant source of signal, contrary to presumptions based on single-channel radar data collected by SIR-B (Stone and Woodwell, 1982). Double bouncing is less significant than in flooded areas because the ground is less reflective of the radar illumination, and volume scattering from the disturbed forest canopy is still significant because the forest canopy was not completely destroyed. Single bounce scattering is large, probably because of the presence of felled tree-trunks. Studies of radar scattering from a layer of randomly oriented, horizontal, dielectric cylinders showed HH-polarized scattering can be very large, if not dominant (Rignot, 1995). In our

decomposition, the presence of felled trees probably translates into a significant increase in single bounce scattering over recent slash and burn compared to other types of land cover. Older clearings show much less double and single bouncing, probably because of the rapid regrowth of the understory vegetation and/or the subsequent removal of the remaining tree trunks.

Analysis of the SAR Classification

We visited 24 fields, and examined differences between Landsat and SIR-C in more than 150 fields based on the history of land use extracted from the SPOT data. We now discuss the results by land cover category. These categories are: 1) open water, 2) flooded dead forests; 3) non-forest; 4) forests; 5) slash and burn; 6) Initial regrowth; 7) Intermediate regrowth; and 8) Advanced regrowth.

Water: Open water has low reflectance in both radar and optical. In the radar data, it is most easily identified as areas of lowest backscatter at HV-polarization, close to the system noise floor (Table 1). Small river streams within the forest are misclassified by SAR due to edge effects from the surrounding forest.

Flooded dead forests: Flooded dead forests are distinctly radar-bright, with large (120 degrees) phase difference between HH- and VV-polarized returns at both C- and L-band (Table 1). They are not separated from open water by Landsat because these forests are dead and have no live biomass. At the exception of one area in the north-east of the scene perhaps misclassified as recent slash and burn, flooded dead forest was correctly classified with SAR throughout the entire scene. Separating those forests from other types of disturbed forests is relevant because their destruction did not result directly from deforestation activities.

Non-forest (no woody biomass): Non-forests are defined differently in the Landsat and SIR-C classifications. In Landsat, Non-forests are defined as bright in band 3 and 5, and correspond on the ground to pasture, bare fields, and slash and burn. In SIR-C, Non-forests are defined as areas of no woody biomass, meaning low HH- and HV-polarized returns at L-band (Table 1), and correspond to pastures, bare fields or small areas of subsistence cultivation.

Areas identified as non-forest by SIR-C are old clearings from 1986, 1988 and 1989. A few stands close to highway 111-364 or along a main access road which were cleared in the summer of 1994 (primary forest in Landsat 1993) had apparently no woody biomass left in October 1994 according to the SIR-C classification. We did not visit those fields, but the results suggest felled tree-trunks must have been removed from the ground.

Several areas identified as Def-forest by Landsat were classified as new clearings with SIR-C. One example area, labeled R6, burned in 1993 and still containing large amounts of woody biomass in 1995, is shown in Figure 4. Both classifications are correct, but SAR helps refine the characteristics of those fields in terms of woody biomass and charcoal residues.

Forests: Forests have a uniform reflectance in the Landsat imagery and are well distinguished from the other classes. In the SAR data, primary forest has the highest level of HV-polarized backscatter (Table 1), indicating high crown biomass, and an intermediate level of brightness at the other polarizations. Textural variations in radar backscatter are more pronounced in the forest than in any other type of land cover (see Table 1). Water is an exception because it is close to the noise floor of the data. Without using texture, forest is however well separated in the SIR-C SAR

data. Errors are mostly commission errors as intermediate regrowth (see below), and slash and burn from 1993 are incorrectly classified as primary forest.

Slash and burn: In the Landsat data, 1-year-old clearings (forest in SPOT 1992) appear blue, because there was not much green vegetation left after clearing. They are classified as non-forest. A few clearings are classified as regrowth, probably because there was enough green vegetation left undisturbed in the field after clearing. Another possibility is understory regrowth from the previous year was significant. SAR identifies <1-year old clearing more easily because of their very bright HH-polarization response and the absence of large phase differences between HH- and VV-polarization. Slash and burn from 1993 is however confused with forest in the SIR-C classification. As hypothesized by Stone and Woodwell (1982), recent clearings start off very bright and decrease in brightness with age. In our data, we find that after one year, confusion with the forest is possible. After > 1 year, confusion is again reduced because these disturbed areas become less bright than the forest. All forest clearings from 1991 and 1992 were correctly separated from the forest and identified either as initial regrowth or HH-forest. Field studies conducted in the near-by city of Jamari by Kaufman et al. (1995) indicated a total biomass consumption of about 50% for slashed primary forests in this region. Based on their results, total above-ground biomass of slash and burn should range from 140 to 220 tons/ha.

Initial regrowth: In Landsat, secondary growth is characterized by a bright reflectance in band 4, moderate to high reflectance in band 5 and low reflectance in band 3. Crops also have moderate to high reflectance in band 5, but low reflectance in band 4. Few crops were present in our study area. In the SIR-C data, secondary regrowth is defined as an intermediate level of woody biomass between non-forest and forest,

with no preferred vertical or horizontal structure as opposed to the case of recent slash and burn. Initial regrowth, 0-5 years of age, probably has a **woody** biomass of the order of 20-50 tons/ha (Uhl et al., 1988).

Intermediate regrowth, typically 7-8 years of age and cleared in 1986 or 1988, was not separated well from the forest by SIR-C SAR, but was correctly identified as secondary growth in the Landsat data, L-band signals do not separate those stands from the forest well because of signal saturation. Cleared between 1986 and 1988, 6 to 8 years prior to the SIR-C flight, those fields have been replaced mostly by cecropia-dominated forests. Their woody biomass is probably in the range 50-100 tons/ha (Uhl et al., 1988). Earlier studies conducted with airborne SARs suggested L-band signals saturate about 100 tons/ha woody biomass (e.g. Dobson et al., 1992). Here, the cecropia forests probably do not have woody biomasses > 100 tons/ha but their canopy of large shedded leaves probably reached a mature stage of crown biomass which explains the saturation of the L-band HV-polarized signals. Landsat TM imagery separates well those areas from primary forest, probably because they contain different tree species.

Advanced regrowth, > 10 year of age, could not be identified by either sensor in our study site. We only found one small area in the time series of SPOT data, next to a large farm settlement. In the SIR-C 1986 data, this forest already had the spectral characteristics of regrowth several years of age. We therefore believe the regrowth was at least 10 years of age in 1994.

SIR-C SAR / Landsat Combined Classification

We combined the classifications produced by both sensors using a simple combinatory

analysis. The results are shown in Figure 8. The definition of each class and the performance of the classification is discussed next by land cover category. We utilized 8 categories of land cover for which we had high confidence in the results. These categories are: 1) open water; 2) flooded dead forest; 3) clearings with no woody biomass; 4) forest; 5) <1-year-old slash and burn; 6) 1-year old slash and burn; 7) initial regrowth; and 8) intermediate regrowth.

Open water was mapped using areas classified as open water by Landsat TM after removing flooded dead forests identified by Silt- SAR. Flooded dead forests were delineated using the SIR-C SAR classification. Non-forest was defined using the areas classified as Non-forest by SIR-C SAR, meaning no woody biomass. Forests were mapped using the Landsat TM classification since SIR-C SAR overestimated the fraction of forest. Slash and burn from 1994 were identified using SIR-C SAR alone. Slash and burn from 1993 were identified as areas classified as forest by Silt- SAR and Non-forest by Landsat TM. Initial regrowth was mapped using the S11- C SAR classification. Finally, intermediate regrowth was identified as areas classified as forest by S11- C SAR and secondary regrowth by Landsat TM.

This combination resulted in major improvements in the characterization of land cover types and in confidence of the classification. In secondary growth, Landsat helped identify live vegetation and S11- C SAR helped categorize different levels of woody biomass. Our preliminary survey was not sufficient to provide quantitative estimates of the classification accuracy of each type of land cover, but the 8 broad types of land cover discussed above were identified with high confidence by both sensors. To obtain a more comprehensive assessment, the analysis will be extended to cover larger areas of Rondonia, and an extensive ground survey is planned in the summer of 1996.

Potential of International SARs

C-band VV (similar to ERS-1 SAR, launched in 1991) does not separate forests from slash and burn (Table 1), and provides only a 2-3 dB contrast between forest and pasture (Table 1), compared to more than 6 dB at L-band (Table 1). Its potential for land applications is limited. C-band HH (similar to Radarsat SAR, launched in 1995) yields bright returns in recent slash and burn of high biomass, and non-forest is better separated from the forest than at C-band VV, but other types of land cover are not well separated from forest. With single date imagery, C-band SARs have limited potential for deforestation studies.

L-band HH (JERS-1 SAR, launched in 1992) could be more appropriate to detect changes in woody biomass. Over the Rondonia test site, JERS-1 SAR (Figure 3) however underestimated the area of deforestation by >100% because forest fallow and undisturbed forests have similar brightnesses. Recent clearings are slightly brighter than the forest. The contrast in radar backscatter is less than in the SIR-C data, probably because the JERS-1 SAR data were acquired later in the season. Clearings identified by JERS-1 SAR correspond to areas of no woody biomass in the SIR-C/Landsat land cover classification. We conclude single-date JERS-1 SAR imagery is likely to underestimate deforestation and may provide only limited information on secondary growth.

None of these single-channel spaceborne SARs were optimized for land cover mapping in the tropics. Long radar wavelengths, with both like and cross polarizations are required for land cover mapping applications in the tropics. Radar wavelengths > 24 cm should probably separate better 7-8 years forest regrowth from primary forests. In the tropical rain-forest of the Manu National Park, in Peru, airborne SAR data

gathered at P-band frequency (68 cm) separated cecropia-dominated successional forests very well from other forest types, and indeed much better than at L- and C-band frequencies (Rignot et al., 1995).

Because the analysis presented here was limited to a single site, we should be careful not to overstate the validity of the results, especially with regards to the apparent saturation of the radar signals in mature forest. Other types of regrowth must be considered, with different tree species, as well as other types of land use, in different regions. For instance, airborne SAR observations of the 2,200-acre farm settlement of Gallon Jug in northern Belize revealed L-band signals could detect crops underneath native trees that remained undetected in Landsat imagery. Although L-band signals seemingly saturate over mature tropical forests, subtle changes in forest structure and even understory vegetation are still likely to be detected very well.

Conclusions

Few studies of the optical/radar synergy have been conducted in the tropics, mostly because of a lack of appropriate radar data. The results of this study suggest the combined use of optical and radar imagery would significantly improve our characterization of land cover types in the tropics, especially with regards to woody biomass and forest structure of disturbed forests. In places often shrouded by clouds, imaging radars may also be the only alternative to Landsat/SPOT imagery.

Prospects for the synergistic utilization of both sensors are currently limited. Existing international SARs are not optimized for land cover applications over highly vegetated terrain. A SAR instrument operating at a long radar wavelength, with both like and cross-polarizations is needed for studying changes in land cover and land use.

Complementary analysis of SIR-C data gathered in other parts of the tropics will shortly follow. These studies will help provide a more extensive evaluation of this new technology for studying tropical land use and for establishing a general methodology and structure for synergistic utilization of both optical and radar instruments.

Acknowledgements

This work was partly carried out at the Jet Propulsion Laboratory, California Institute of Technology, under a contract with the National Aeronautics and Space Administration. The authors would like to thank Walter Chomentowski for assistance in the preliminary field survey, the Landsat Pathfinder project and the IGBP-DIS projects for providing the Landsat and SPOT data, and all the people at the Jet Propulsion Laboratory involved with the processing and generation of the SIR-CSAR products.

References

- Adams, J.B. and 6 others (1995), Classification of multispectral images based on fractions of endmembers: Application to land-cover change in the Brazilian Amazon, *Rem. Sens. Environ.* 52, 137-154.
- Alves, D. S. and D.L. Skole (1996), (characterizing land cover dynamics using multi-temporal imagery, *Int. J. Rem. Sens.*, in press.
- Brown, S. and A.F. Lugo (1990), Tropical secondary forests, *J. of Tropical Ecology* 6, 1-32.
- Dale, V.J., R.V. O'Neill, M. Pedlowski, and F. Southworth, (1993) Causes and effects of land-use change in central Rondonia, Brazil, *Photogramm. Eng. Rem. Sens.* 59(6), 997-1005.
- Durden, S.L., J.J. van Zyl and H.A. Zebker (1989) Modeling and observation of the radar polarization signature of forested areas, *IEEE Trans. Geosc. Rem. Sens.* 27(3), 290-301.
- Dobson, M. C., F.T. Ulaby, J. LeToan, A. Beaudoin, E.S. Kasischke, and N. Christensen, (1992), Dependence of radar backscatter on conifer forest biomass, *IEEE Trans. Geosc. Rem. Sensing* 30, 412-415.
- Houghton, R.A. and D.L. Skole (1990), Carbon, in B.L. Turner et al. (eds.), *The Earth As*

Transformed by Human Action, Cambridge University Press, Cambridge, U. K., 393-408.

Houghton, R.A. (1991), Tropical deforestation and atmospheric carbon cycle, *Clim. Change* 19, 99-118.

Houghton, R. A., D.L. Skole, and J. S. Lefkowitz (1991) Changes in the landscape of Latin America between 1850 and 1985: II a net release of CO₂ into the atmosphere, *J. Forest Ecology and Management* 38, 133-199.

Kauffman, J.B., D.L. Cummings, D.E. Ward, and R. Babbit (1995) Fire in the Brazilian Amazon: 1. Biomass, nutrient pools, and losses in slashed primary forests. *Oecologia* 104, 397-408.

Lucas, R. M., M. Honzak, G.M. Foody, P.J. Curran and C. Corves (1993) Characterizing tropical secondary forests using multi-temporal Landsat sensor imagery, *Int J. Rem. Sens.* 4(16), 3061-3067.

Malingreau, J.P. and C.J. Tucker (1988) Large-scale deforestation in the southeastern Amazon basin of Brazil, *Ambio* 17(1), 49-55.

Moran, E.F., E. Brondizio, P. Mausel and Y. Wu (1994) Integrating Amazonian vegetation, land-use, and satellite data, *Bioscience* 44(5), 329-338.

Neftel, A., E. Moor, J. Oeschger, and B. Stauffer (1985) Evidence for polar ice cores for the increase in atmospheric CO₂ in the past two centuries, *Nature* 315, 45-47.

Nepstad, D.C., C. Uhl and E.A.S. Serrao (1991), Recuperation of a degraded Amazonian landscape: forest recovery and agricultural restoration, *Ambio* 20, 248-255.

O'Neill, P. (1993) New sensors eye the rain forest, *National Geographic* Sept. 93, 118-130.

Rignot, E. (1995), A Model for Interpreting the Unusual Radar Echoes from the Greenland Ice Sheet, *J. Geophys. Res.* 100(15), 9389-9400.

Rignot, E. and R. Chellappa, (1992) Segmentation of polarimetric synthetic aperture radar data, *IEEE Trans. Imag. Proc.* 1, 281-300.

Rignot, E., R. Zimmerman, J. van Zyl and R. Oren, (1995) Spaceborne applications of a P-band imaging radar for mapping of forest biomass, *IEEE Trans. on Geosc. Rem. Sens.* 33(5), 1162-1169.

Sader, S.A. (1987) Forest biomass, canopy structure, and species composition relationships with multipolarization L-band synthetic aperture radar data, *Photogramm. Eng. Rem. Sens.* 53(2), 193-202.

Sader, S. A., R.B. Waide, W.T. Lawrence and A.'J'. Joyce (1989) Tropical forest biomass and successional age class relationships to a vegetation index derived from Landsat TM data, *Rem. Sens. Environ.* 28, 143-156.

Skole, D.L. and C. J. Tucker (1993) Tropical deforestation and habitat fragmentation in the Amazon: satellite data from 1978 to 1988, *Science* 260, 1905-1910.

Skole, D.L., W. H. Chomentowski, W.A. Salas, and A.J. Nobre (1994) Physical and human dimensions of deforestation in Amazonia, *Bioscience* 44(5), 314-321.

Steininger, M.K. (1996), Tropical Secondary forest regrowth in the Amazon: age, area and change estimation with Thematic Mapper data, *Int. J. Rem. Sens.* 17(1), 9-27.

Stone, T.A. and G.M. Woodwell (1988) Shuttle imaging radar A analysis of land use in Amazonia, *Int. J. Rem. Sens.* 9(1), 95-105.

Tou, J.'J'. and R.C. Gonzalez (1974) Pattern Recognition Principles. Reading, Massachusetts: Addison-Wesley Publishing Co.

Townshend, J. R. G. and C.(). Justice (1988), Selecting the spatial resolution of satellite sensors required for global monitoring of land transformations, *Int. J. Rem. Sens.* 9(2), 187-236.

Tucker, C. J., B. N. Holben and 'J'. E. Goff, (1984) Intensive forest clearing in Rondonia, Brazil, as detected by satellite remote sensing, *Rem. Sens. of Envir.* 15, 255-261.

Uhl, C. R. Buschbacher, and E. A. S. Serrao (1988) Abandoned pastures in eastern Amazonia. 1. Patterns of plan succession, *J. Ecology* 76, 663-681.

van Zyl, J. J. (1992) Application of Cloude's target decomposition theorem to polarimetric imaging radar data, *Proc. SPIE* Vol. 1748 Radar Polarimetry, pp. 184-191.

van Zyl, J. J. (1989) Unsupervised classification of scattering behavior using radar polarimetry data, *IEEE Trans. Geosc. Rem. Sens.* 27(1), 36-45.

Table 1. Radar characteristics of the 8 training areas used for the SIR-CSAR land cover classification. σ_{HV}^o is the radar cross-section expressed in dB at HV-polarization. ρ_{HHVV} is the normalized correlation coefficient between HH- and VV-polarized radar returns, and ϕ_{HHVV} is the phase difference between HH- and VV-polarized radar returns expressed in degrees.

Band	σ_{HH}^o	σ_{HV}^o	σ_{VV}^o	ρ_{HHVV}	ϕ_{HHVV}	Land Cover Type
L-						
	-19.5	-29.8	-18.3	0.42	-5	Open water
	-10.6	-20.8	-11.0	0.55	10	Clearings no biomass
	-9.2	-18.9	-11.0	0.46	10	Clearings no biomass
	-4.4	-17.7	-9.0	0.40	-120	Flooded dead forest
	-5.8	-15.8	-8.3	0.38	-5	Initial Regrowth
	-6.0	-13.9	-8.2	0.31	-15	Initial Regrowth
	-5.2	-13.9	-7.4	0.40	-5	Slash and burn
	-7.4	-12.1	-7.4	0.29	0	Primary forest
C-						
	-16.4	-24.1	-16.7	0.27	-15	Open water
	-3.9	-11.9	-5.8	0.46	0	Clearings no biomass
	-4.8	-11.6	-5.5	0.46	0	Clearings no biomass
	-1.8	-17.1	-7.7	0.35	-130	Flooded dead forest
	-3.2	-13.3	-5.3	0.54	0	Initial Regrowth
	-4.0	-10.4	-4.6	0.42	-5	Initial Regrowth
	-3.2	-11.2	-4.4	0.49	-5	Slash and burn
	-4.7	-10.5	-4.7	0.46	0	Primary forest

List of Figures

Figure 1. False color composite image of the study site in the state of Rondonia, Brazil, acquired by SIR-C; on October 7, 1994. L-band HH is red, L-band HV is green, and C-band HV is blue.

Figure 2. False color composite image of the study site in Rondonia acquired by Landsat TM on October 7, 1993, Band 4 is red, band 3 is green, and band 5 is blue.

Figure 3. JERS-1 SAR scene of the test site acquired in February 1994

Figure 4. Examples of land cover types at test site. (a) Photo of 1993 clearing with regrowth from 1989 in background and 1 year regrowth in foreground (8). (b) initial rough clearing (R6) (c.) Clearing classified as secondary growth by Landsat (TM). (d) 1995 clearing.

Figure 5. classification map of the Landsat TM 1993 data.

Figure 6. Classification map of the SIR-C 1994 data.

Figure 7. Mathematical decomposition of the radar scattering for the Rondonia test site at (a) C-band and (b) L-band frequencies. Red is the amplitude of double bouncing interactions, green is volume scattering, and blue is single bouncing.

Figure 8. Classification of land cover type using SIR-C SAR and Landsat TM data. combined



Figure 1. Rignot, Salas and Skole, 1996



Figure 2.

Rignot, Salas and Skole, 1996



Figure 3. Rignot, Salas and Skole, 1996

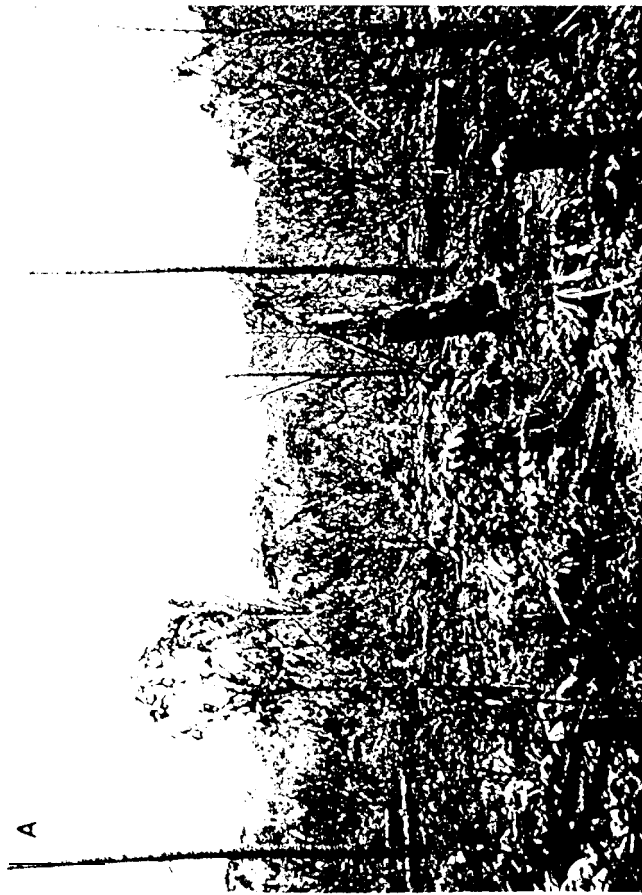


Figure 4 R gnot, Salas and Skole, 1996

- Open Water
- Pfirmclry forest
- NorT forest
- f<cgfowttl



Figure 5.

Rignot, Salas and Skole, 1996

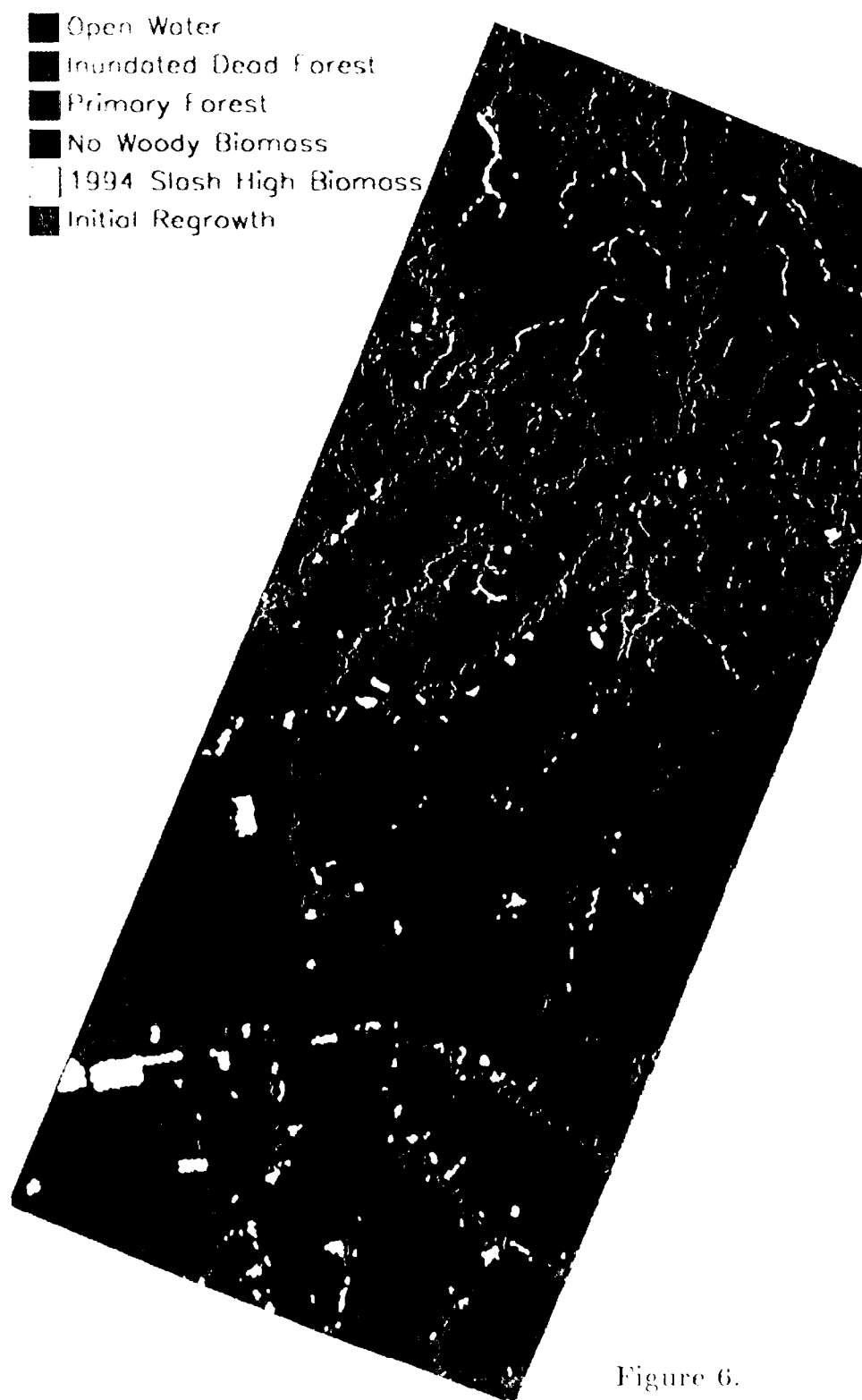


Figure 6.

Rignot, Salas and Skole, 1996

- **skqle!** Bouncing
- DoubleBouncing
- volufrle Scottering

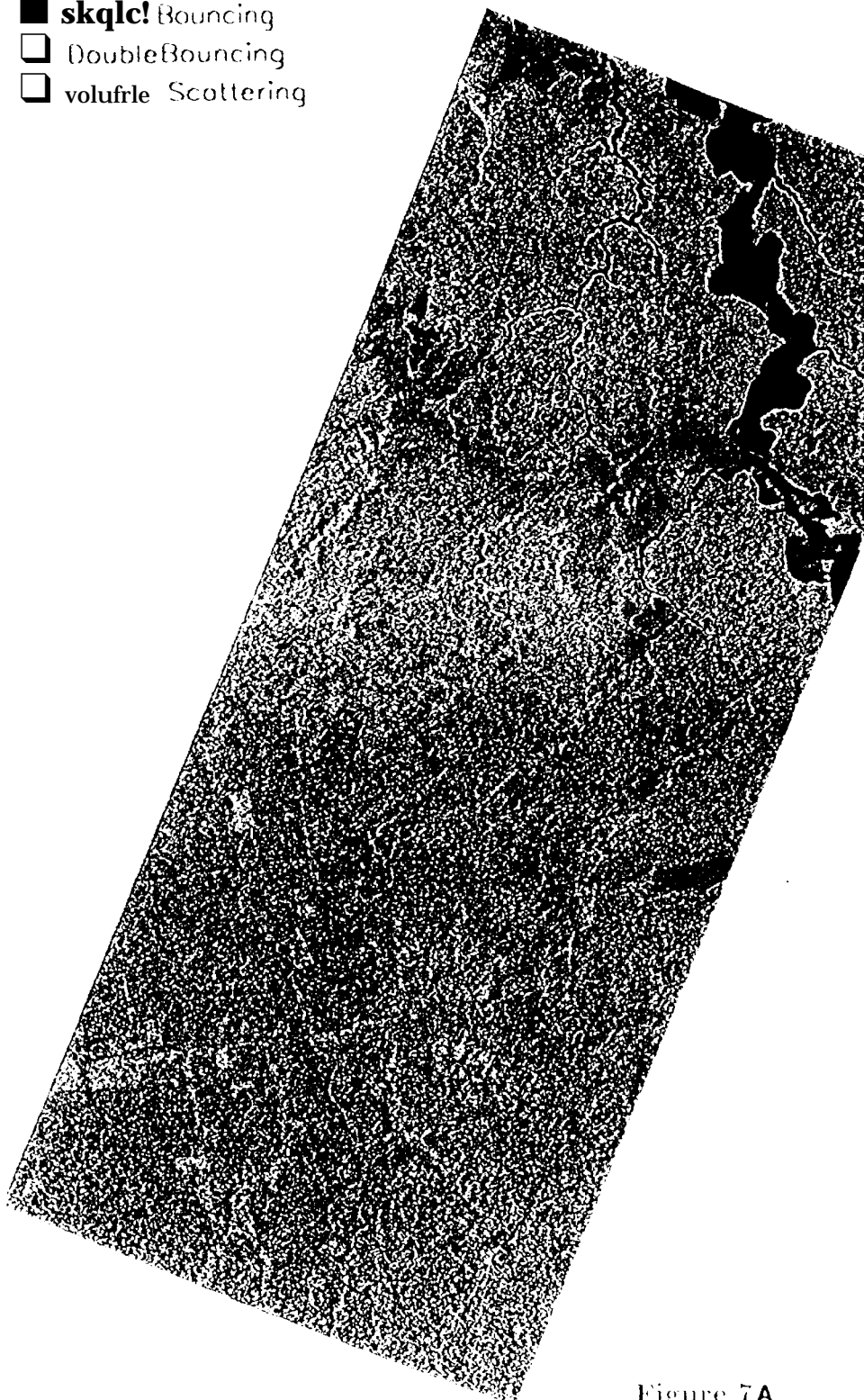


Figure 7A

Rignot, Salas and Skole, 1996

- SingleBouncing
- DoubleBouncing
- Volume Scottering

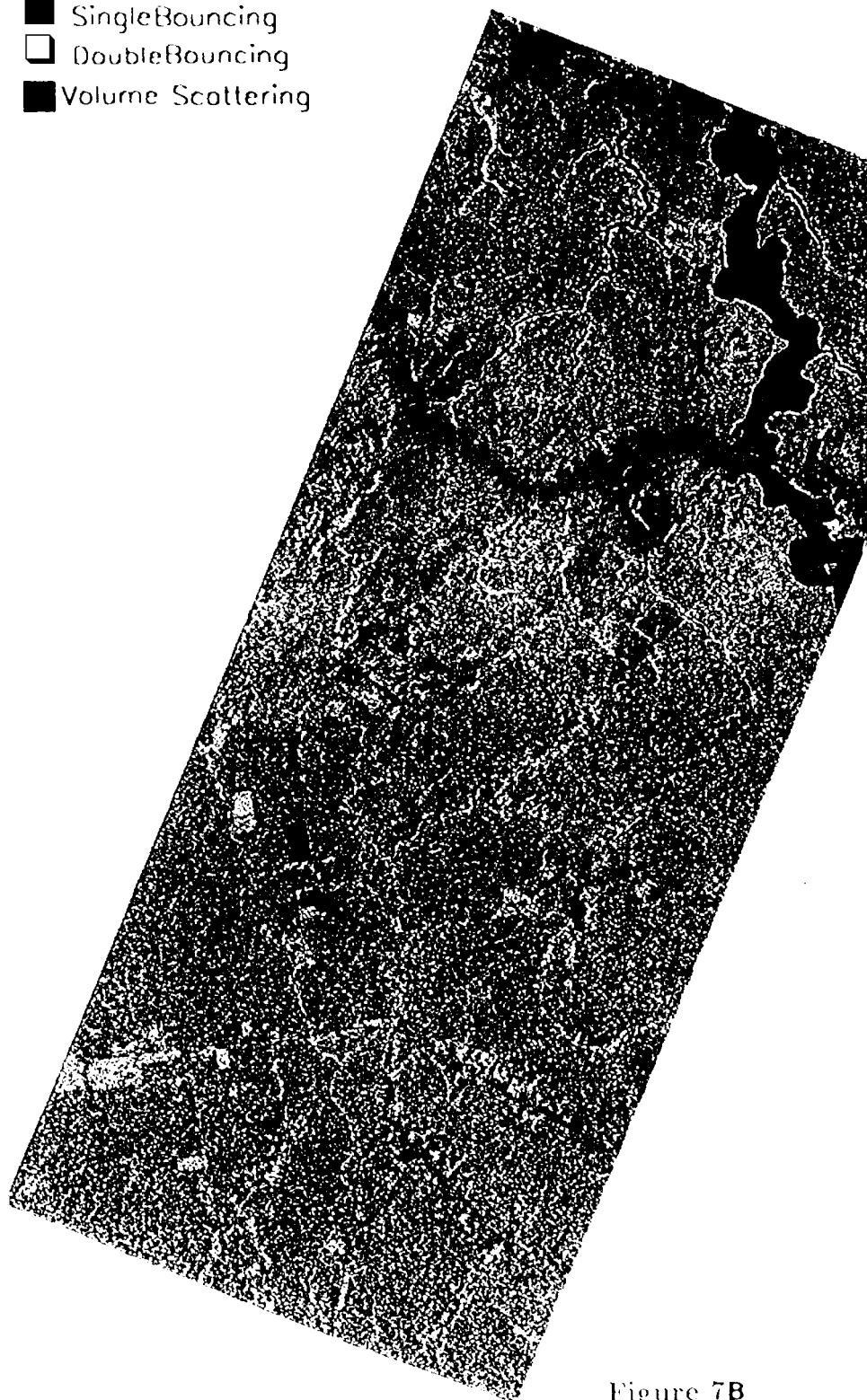


Figure 7B

Rignot, Salas and Skole, 1996

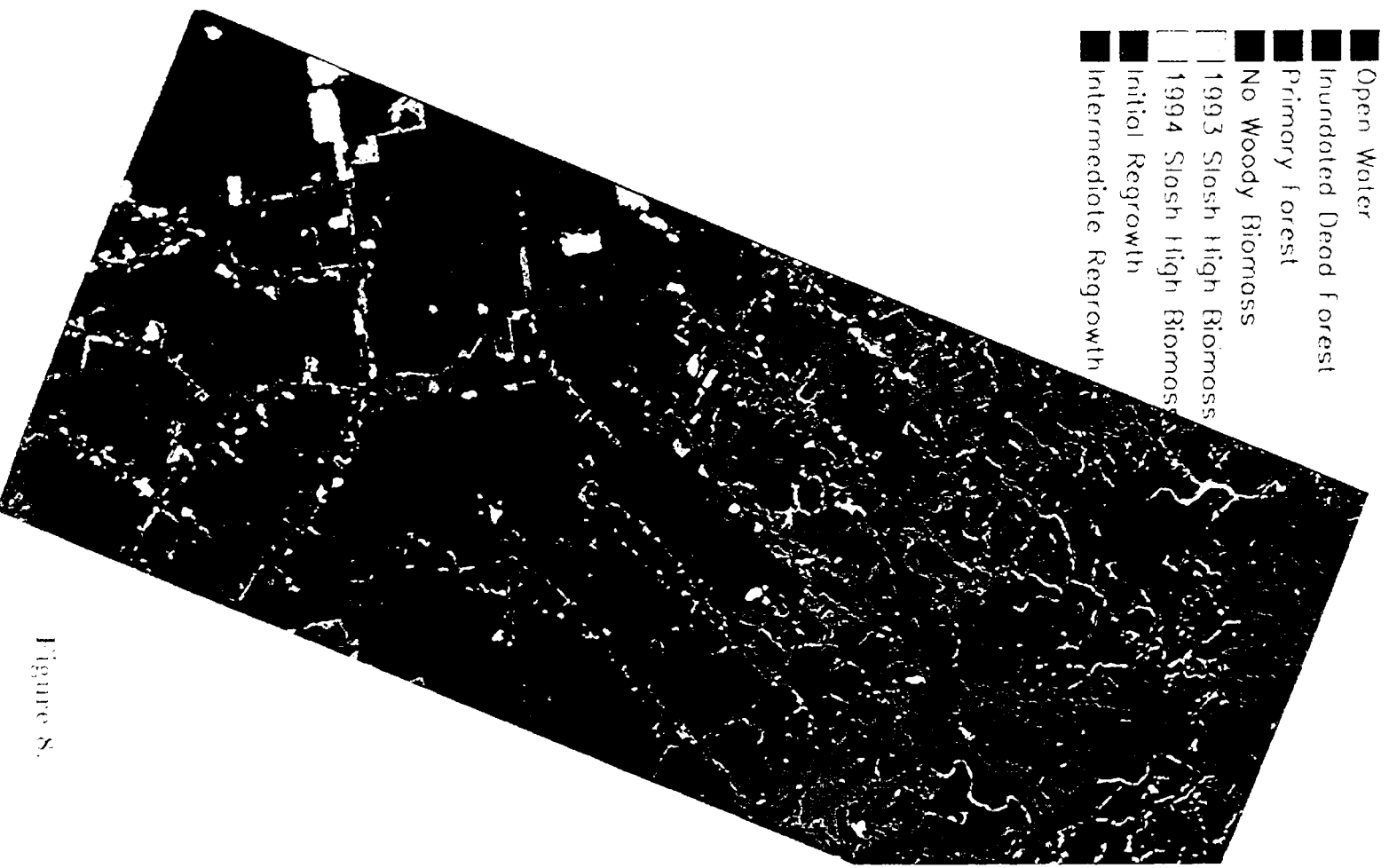


Figure 8.